

## Chirality of Large Random Supramolecular Structures\*\*

Omer Katzenelson, Hagit Zabrodsky Hel-Or, and David Avnir\*

**Abstract:** The structural chirality of large, random supramolecular structures, spiral diffusion-limited aggregates, is analyzed and studied in detail by using a continuous chirality measure. It is found that classical definitions and terminologies of chirality are too restrictive for the description of such complex objects. A refined methodology and a conceptual vocabulary are developed, along with a generalized definition of chirality. Their application is demonstrated in detail on these large structures. The classical definition of chirality, tailored for small, nonrandom species, is a limiting case of the generalized viewpoint we propose.

## Keywords

chirality · diffusion-limited aggregates  
· structural chemistry · supramolecular structures

## Introduction

**Comments on the Definition of Chirality:** "I call any geometrical figure, or any group of points, *chiral*, and say it has *chirality*, if its image in a plane mirror, ideally realized, cannot be brought to coincide with itself" (Kelvin, 1884).<sup>[1]</sup> This 111 year old definition held remarkably well over the decades of evolution of structural chemistry (see Prelog's definition in his Nobel lecture,<sup>[2]</sup> cited below) and is still used routinely today. The recent intensive research into disordered and semi-ordered structures (polymers and oligomers, aggregates, clusters, liquid crystals, and other supramolecular structures), many of which are chiral,<sup>[3–5]</sup> led us to re-explore some conceptual aspects of chirality associated with such structures. We find that while the classical definition of chirality is well suited to deal with small molecules, it fails in the accurate description of large random structures. We point out explicitly the inadequacies of the classical definition, and show that this definition is a limiting case of much broader concepts, which are needed to encompass the structural richness of both small molecules and supramolecular structures.

We concentrate here on aggregate structures of the type shown in Figure 1a; however, the questions, arguments, and proposed solutions presented below are general. This aggregate (Fig. 1a) has perhaps been the most studied random structure,<sup>[6]</sup> known in short as DLA (diffusion-limited aggregate); it represents a very wide variety of both growth (polymerizations, coagulations, electrodepositions, surface island formations, etc.) and disintegration phenomena (dissolution, forced penetration, etc.).<sup>[7]</sup> A simple algorithm for obtaining the DLA is to build one particle after the other, letting the particle diffuse and stick to the growing structure.<sup>[6, 7]</sup> Although entirely random, the DLA in Figure 1a is chiral under Kelvin's definition: it does



Fig. 1. a) A diffusion-limited aggregate (DLA) and b) its mirror image. The DLA (a) is incidentally chiral and its enantiomer (b) virtual.

not coincide with its two-dimensional (2D) mirror image (mirror line, in 2D), shown in Figure 1b. Since we realized the nontriviality associated with chirality of an entirely random nature (c.f. Ruch's potato<sup>[8]</sup> and Mislow's discussion of the chirality of large ensembles<sup>[9]</sup>), we first decided to create DLAs in which chirality is inherent. There are a number of ways in which this can be done;<sup>[10, 11]</sup> one of them is to bias the diffusional pathways of the aggregating particles from purely Brownian to chiral.<sup>[11]</sup>

For instance, if clockwise diffusion is (partially) favored over counterclockwise diffusion, a chiral object reflecting this bias will form. The way in which we actually do this is described below, but at the moment let us concentrate on a typical result, shown in Figure 2a, depicting a clearly chiral DLA. It should be noted, however, that induction of macroscopic chirality need not be the result of a continuous external bias; initial fluctuations are enough, as shown both by experiment<sup>[12]</sup> and simulation.<sup>[13]</sup> We emphasize that chiral clusters and aggregates have indeed been observed experimentally,<sup>[4, 14, 15]</sup> and that the principles of the structural analysis described below are directly applicable to the patterns observed in these experiments. The DLAs shown in Figures 1 and 2 raise the following problems:

**Problem 1:** What is the enantiomer of the chiral DLA shown in Figure 2a? Figure 2b shows an artificial reflection of 2a. The problem is that, being formed in a random process, not only can

[\*] Prof. D. Avnir, Dr. H. Zabrodsky Hel-Or, O. Katzenelson  
Institute of Chemistry, The Hebrew University of Jerusalem  
Jerusalem 91904 (Israel)  
Telefax: Int. code + (2) 652-0099  
e-mail: david@granite.fh.huji.ac.il

[\*\*] Continuous Symmetry Measures, Part V. Part IV, ref. [21].

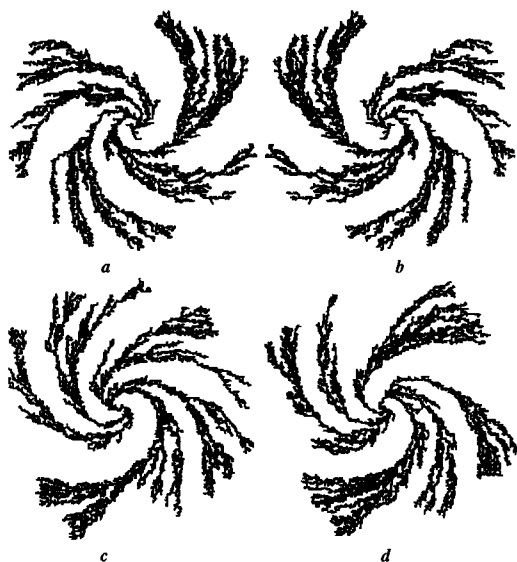


Fig. 2. Chiral DLAs. a) One way of obtaining such structures is to take the DLA in Figure 1 and rotate it clockwise against friction around its center; we therefore assign it the symbol (*R*) [16]. b) The virtual (*S*) enantiomer of (a). c) and d) two natural (*S*) enantiomers of (a).

the structure in Figure 2a never be repeated, but, in principle, the enantiomer in Figure 2b can never form. What then is the meaning of chirality of an object that can never have an exact enantiomer?

**Problem 2:** For the sake of further discussion, let us refer to the reflected shape of the random object as the *virtual enantiomer* (both Figs. 1b and 2b) and the object obtained by the same random process, only biased in the opposite (enantiomeric) direction, as the *natural enantiomer*, shown in Figure 2c (new terminology is collected in Appendix A). There is an *infinite number* of natural left-handed enantiomers (e.g., Figs. 2c and 2d)<sup>[16]</sup> for each right-handed structure (Fig. 2a). What is then the meaning of an enantiomeric pair when each member of this pair has an infinite number of distinctly different structures, and, taking a single member of the infinite group of clockwise (*R*) enantiomers, how justified would we be in picking out any one of the infinite counterclockwise (*S*) structures and calling the chosen structures, which are definitely not reflections of each other, an enantiomeric pair?

#### Abstract in Hebrew:

#### הכיראליות של מבנים אקראיים על-מולקולריים

עמר כצנלסון, חגית זברודסקי-הל-אור ודוד אבנר,  
המחלקה לכימיה אורגנית, האוניברסיטה העברית בירושלים.

**תקציר:** הכיראליות של מבנים אקראיים על-מולקולריים (צברים ספירליים) נלמדת ונבחנת לפרטיה, על-ידי שימוש במודל רציף לכיראליות. נמצא, שהגדרות ומונחים קלאסיים של כיראליות מוגבלים מכדי לתאר מבנים מורכבים כאלה. פותחו שיטה מתקנת ומילון מושגים, וכן הורחב מושג הכיראליות. הגישה של אלה מודגם בהרחבה על הצברים הספירליים. הגישה הקלאסית לכיראליות הינה מקרה פרטי של הגישה המוכללת שאנו מציעים.

**Problem 3:** Coming back to the DLA in Figure 1a and to the very fact that it is chiral because it is random, how can one differentiate between *incidental* (Fig. 1a) and *inherent* chirality (Figs. 2a, 2c, 2d)? What is it that makes incidental chirality distinctly different, at least by intuition, from inherent chirality? Is there place at all for a distinction? Should one refer to objects that are incidentally chiral (almost any object around us) in terms of chirality at all?

**Problem 4:** We termed the structures in Figures 2c and 2d natural enantiomers of 2a. Since their structures are different in detail, how can one *quantitatively* assess whether the *chirality content* of structures (Figs. 2b–d) are similar? Furthermore, Figure 3 shows a series of DLAs with clearly changing spirality character. How can this be measured?

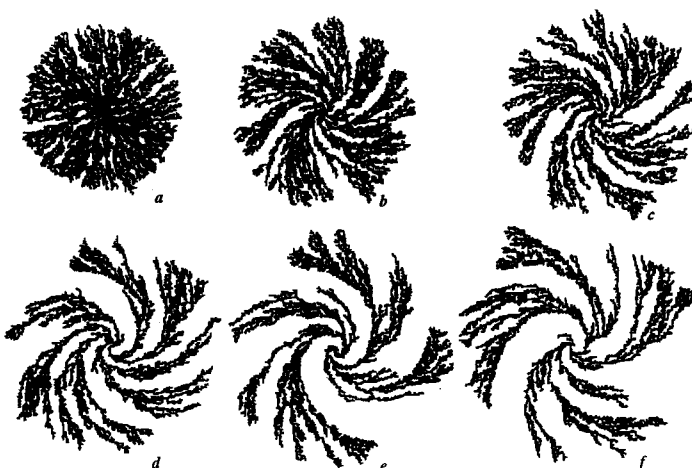


Fig. 3. The degree of chirality can be controlled by varying the construction parameters of the structure (see text). Here,  $N = 10^4$ ,  $p = 1.0$ , and  $\Delta r = 0.2$  were kept constant, while  $\Delta a$  was varied as follows: a) 10, b) 22, c) 30, d) 50, e) 70, and f) 90.

**Problem 5:** Whenever large detailed objects are analyzed, the question of resolution of measurement is obvious. Thus, whereas the chirality of the equilibrium structure of, say, 2-iodobutane is uniquely defined because all information on the positions of all the nuclei is given quite accurately, the situation with, say, proteins is different: their structures can be determined at various degrees of resolutions. Our fifth problem therefore concerns the dependency of chirality on *resolution*. This problem (c.f., Mezey's treatment of resolution-based chirality and similarity measure)<sup>[17]</sup> is intimately linked to the next one.

**Problem 6:** The building blocks of the chiral DLAs are not chiral (square pixels, in our case); yet the whole structure is (for experimental observations, see ref. [4]). Where is the transition from achirality to chirality? What is the minimum size of features that contribute to the chirality of the whole? (the equivalent question for small molecules is to ask where the chiral center is.)

**Problem 7:** An interesting phenomenon observed in many artificial and natural random objects, which has been the center of intensive studies in the past 15 years, is that many of their properties scale isotropically with size as a power law.<sup>[7]</sup> For instance, in DLAs the mass ( $m$ ) scales with the radius ( $r$ )<sup>[6]</sup> according to Equation (1), where  $D$  is the mass fractal dimension

$$m \approx r^{-D} \quad (1)$$

sion. It has been shown that an approximate geometric interpretation of Equation (1) is in terms of an invariance to scale;<sup>[6]</sup> in other words, a large DLA (with  $r_1$ ) and a small DLA (with  $r_2$ ) are indistinguishable when the large DLA is reduced in size from  $r_1$  to  $r_2$ . Later on we show that chiral DLAs obey Equation (1) as well, that is, they are symmetric to scale transformations. With this in mind, let us now examine Prelog's definition of chirality:<sup>[2]</sup> "An object is chiral if it cannot be brought into concurrence with its mirror image by translation and rotation". The two transformations in this definition are symmetry operations; but so is the change of scale for self-similar objects—the symmetry operation is then a dilation/contraction. Should Perlog's definition not be extended to "translation, rotation, and scaling"?<sup>[18]</sup> Are the objects in Figures 2a and 5a, which only differ in size ( $10^4$  and 22880 particles, respectively), but are otherwise constructed with the same parameters, an enantiomeric pair?

## Methodology

**1. Continuous Chirality Measure:** A central tool that we use to formulate, apply, and analyze the conceptual questions raised in the Introduction on a quantitative level is the measurement of the chirality content on a continuous scale. As the methodology has been described in great detail in a recent series of publications,<sup>[19–21]</sup> only a brief outline will be provided here. The method of measurement of chirality is part of a more general approach for the evaluation, on a continuous scale, of the symmetry content of any configuration of points  $P_i$  with respect to any symmetry element or symmetry group. Basically, one searches for the minimum movement that the set of vertices  $P_i$  has to undergo (from  $P_i$  to  $\hat{P}_i$ ) in order that the set of vertices  $\hat{P}_i$  has the desired symmetry  $G$ . The symmetry measure of the set  $P_i$  with respect to  $G$  is then defined by Equation (2). The scale

$$S(G) = \frac{100}{n} \sum_{i=1}^n ||P_i - \hat{P}_i||^2 \quad (2)$$

is bound between zero (the configuration has the desired symmetry) and 1, and the factor of 100 is used for convenience. The latter limit arises as a result of the standard scaling of the size of the configuration to 1 (center of mass to the farthest point) and is obtained when the nearest object with the desired symmetry is a center point; this is the case, for example, when calculating the amount of hexagonality,  $C_6$ , in a perfect pentagon. However, since translation to a nearest plane is shorter than translation to a center point, we find that  $S$  with respect to mirror symmetry  $\sigma$  is always smaller than the maximum possible value of 1 (or 100, on the expanded scale).

$S(G)$  also serves as a measure of chirality, if one takes  $G$  as a symmetry group containing the identity element  $E$  and an improper symmetry element. In the majority of cases we found<sup>[21]</sup> that the nearest achiral group is simply composed of the elements  $E$  and  $\sigma$ . In 2D (all examples in this report), the nearest achirality is always associated with a reflection line, which we denote as  $\sigma$  too. We shall therefore look for the minimum  $S(\{E, \sigma\})$ , denoted for short as  $S(\sigma)$ .

The main issue with Equation (2) is how to find the nearest set of  $\hat{P}_i$ 's. A general algorithm towards this goal was developed and is described in detail in ref. [20–22], along with a proof that the  $S(G)$  thus obtained is indeed a minimum. Variations on the central theme of that algorithm are possible for various specific cases.<sup>[21]</sup> In our case it is sufficient to analyze the contour of the DLA, which is possible because contour and mass coincide in

these structures.<sup>[6]</sup> The example in Figure 4 captures most of the relevant elements of the method: The object to be symmetrized (Fig. 4a) is converted to a necklace of an even number of

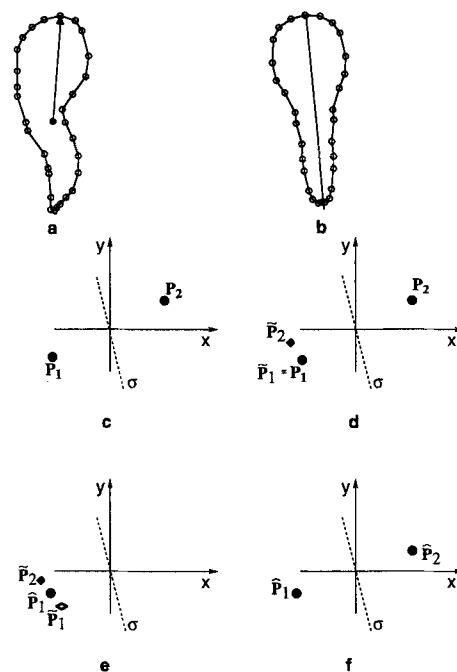


Fig. 4. a) A contour composed of 30 points  $P_i$  (the size is scaled to 1 as shown by the arrow). b) The nearest  $\sigma$ -symmetric  $\hat{P}_i$  to (a). c)–f) Evaluation of the  $S(\sigma)$  value for a pair of points  $P_1/P_2$  with respect to a given mirror line.  $P_1/P_2$  (c) are folded (d) to  $\hat{P}_1/\hat{P}_2$ , averaged (e) to  $\hat{P}_1$  and unfolded (f) into the  $\sigma$ -symmetric pair  $\hat{P}_1/\hat{P}_2$ .

boundary points  $P_i$ , as dense as desired ( $N = 30$  points in our case). Its center of mass is then determined and placed at the origin, and the distance from that center to the farthest  $P_i$  is scaled to 1 (Fig. 4a). The aim is to find the nearest set of  $\hat{P}_i$ 's that is  $\sigma$ -symmetric, that is, to find the reflection line that will cause the set of  $P_i$ 's to move minimally to the set  $\hat{P}_i$ 's (Fig. 4b). Elsewhere we showed that the procedure employed here does not translate the object,<sup>[20, 22]</sup> that is, the center of mass of the set  $P_i$  coincides with the center of mass of  $\hat{P}_i$ . This means that the elements of the group are centered at the origin as well, and the best  $\sigma$  must pass through it.

In the symmetrized object, each  $\hat{P}_i$  must have a  $\sigma$ -symmetric counterpart  $\hat{P}_{N-i}$  across the reflection line (or it must be located on the reflection line). The full set of  $P_i$ 's is divided into subsets of two points, and all possible divisions are tested (points on the reflection line are duplicated). Here is how a pair of points  $P_1/P_2$  are  $\sigma$ -symmetrized with respect to a given  $\sigma$  (Fig. 4c–f):

- 1)  $E$  operates on  $P_1$  and it remains in place ( $P_1 \equiv \hat{P}_1$ );  $\sigma$  operates on  $P_2$  forming the reflected  $\tilde{P}_2$ ; a pair of adjacent points,  $\tilde{P}_1$  and  $\tilde{P}_2$ , is obtained (Fig. 4c–d). We term the step of applying the elements on the vertices the *folding* step. The essence of our methodology is to minimize the distance between  $\tilde{P}_1$  and  $\tilde{P}_2$ . In higher symmetry groups the cluster is much larger. For instance, in order to find the tetrahedrality measure ( $S(T_d)$ ), a cluster of 24 points (the number of the element in the group) is formed and minimized (see ref. [20] for details).
- 2) The folded points  $\tilde{P}_1$  and  $\tilde{P}_2$  are *averaged* to  $\hat{P}_1$  (Fig. 4e), and  $\hat{P}_1$  is *unfolded* (Fig. 4f) by applying the elements of the group to it:  $E$  leaves it in place and  $\sigma$  forms  $\hat{P}_2$  across the reflection line; the pair  $\hat{P}_1/\hat{P}_2$  is  $\sigma$ -symmetric, and the sum of distances  $||P_1 - \hat{P}_1||^2 + ||P_2 - \hat{P}_2||^2$  is minimal (for proofs see previous parts in this series<sup>[21]</sup>). Minimization is performed by

screening over all possible divisions into opposite pairs, that is, over all inclinations of  $\sigma$  (below we shall see that sweeping over all  $\sigma$ 's yields a profile with several local minima). Figure 5 shows what a  $\sigma$ -symmetrized DLA looks like. The rotational symmetry content,  $S(C_n)$  of DLAs, is briefly commented on in Appendix C.



Fig. 5. A DLA (a) and the nearest  $\sigma$ -symmetric shape (b) of its envelope ( $S(\sigma) = 3.06$ ).

**2. The Construction and Properties of Aggregates with Varying Degrees of Chirality:** Diffusion-limited aggregates (DLAs) were built by standard procedures, described many times in the literature.<sup>[6, 7]</sup> As explained in the Introduction, one particle after the other randomly diffuse to a growing cluster and stick to it upon collision; this procedure results in *incidental* chirality (Fig. 1), and *inherent* chirality is induced in the structure when the diffusion of the random walker is chirally biased.<sup>[11, 13, 14]</sup> In our application, the chiral bias is a probability of moving clockwise or counterclockwise along a spiral in each step of the random walk as shown in Figure 6. The spiral we selected is a



Fig. 6. a) A trace of  $1.45 \times 10^5$  random-walk steps. b) A trace of a spirally biased random walk ( $4.0 \times 10^4$  steps). These are two paths from an external starting point to the growing seed.

logarithmic one,<sup>[23]</sup> in which the angle of rotation of the spiral  $\phi$  is related to the radius  $r$  by Equation (3), where  $K$  is a phase

$$\phi = K + c \log r \quad (3)$$

shift and  $c$  is the spiral curvature. For computational convenience we build this spiral by a recursive procedure, in which motion along a spiral line from  $x_n, y_n$  to  $x_{n+1}, y_{n+1}$  is achieved by changing the radius with an incremental radial translation  $\Delta r$  and by an angular translation  $\Delta a$ , according to Equation (4), where  $\phi = \arctg(y_n/x_n)$ ,  $r_n = ((x_n^2 + y_n^2))^{1/2}$  and  $r_i$ , the

$$\begin{aligned} x_{n+1} &= (x_n + \cos(\phi + \Delta a))(r_n + \Delta r)r_i^{-1} \\ y_{n+1} &= (y_n + \sin(\phi + \Delta a))(r_n + \Delta r)r_i^{-1} \end{aligned} \quad (4)$$

position to which  $r_n$  is shifted by the angular translation  $\Delta a$ , is  $((x_n + \cos(\phi + \Delta a))^2 + (y_n + \sin(\phi + \Delta a))^2)^{1/2}$ . In Appendix B we demonstrate that Equations (3) and (4) lead to the same

spiral and show some of its other properties. The shape of the spiral is determined by the values of  $\Delta a$  and  $\Delta r$ . Basically, as  $\Delta r$  or  $\Delta a$  increase (up to  $\approx 90^\circ$  for the latter), the spiral spreads out faster (this is equivalent to increasing  $c$  in Eq. (3)).

## Results and Discussion

**1. The Properties of Chiral DLAs:** The shape of the chiral DLA is dictated both by the shape parameters of the underlying spiral direction ( $\Delta r$ ,  $\Delta a$ ) and by the probability  $p$  of moving in that direction. Figure 3 shows how chirality becomes more pro-

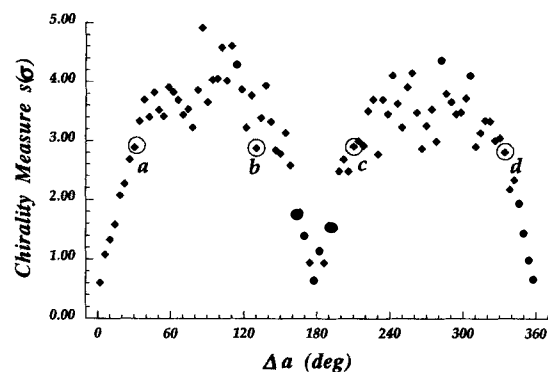


Fig. 7. Quantitative evaluation of the degree of chirality of the DLAs in Figure 3, and the relation between the chirality measure  $S(\sigma)$  and the structural parameter  $\Delta a$ . Points a, b, c, and d are isochiral. Points a and b are homochiral, as are c and d. Points a, b are enantiomers of points c, d.

nounced in a series of DLAs built from  $N = 10^4$  particles, by changing  $\Delta a$  while keeping all other parameters fixed ( $p = 1.0$ ;  $\Delta r = 0.2$ ). Our methodology allows this visual increase in chirality to be expressed on a quantitative level, as shown in Figure 7. Here,  $S(\sigma)$  is plotted as a function of  $\Delta a$ , and it can be seen that the chirality value increases with  $\Delta a$  up to a maximum at  $\Delta a = 90^\circ$  where the spiral curvature is at a maximum, beyond which it drops to a minimum at  $\Delta a = 180^\circ$ ; the cycle then repeats itself in the  $180$ – $360^\circ$  range. The minima do not reach zero, but rather a small chirality value typical of incidental chirality; we return to this point below. Except at the extrema, there are four *isochiral* DLAs (DLAs with the same  $S(\sigma)$  value) in one full cycle of  $360^\circ$ : a and b are separated by  $\pi - 2\Delta a$  and are enantiomers of the same handedness (homochiral), as are c and d. The pairs {a, b} and {c, d}, separated by  $\pi$ , are *natural* enantiomers of each other: a is an enantiomer (and not the enantiomer, as in the language for small molecules) of c and/or d.

Figure 8 shows how the chirality content of the DLAs is controlled by two other structural parameters. Figure 8 (top) shows the relation between  $S(\sigma)$  and  $\Delta r$ : as  $\Delta r$  increases, the curling of the spiral opens, and the chirality of the DLA decreases. Figure 8 (bottom) shows the effect of changing the magnitude of the probability  $p$  on movement along the spiral path: as expected  $S(\sigma)$  increase with  $p$ , showing high sensitivity to changes in  $p$  at low  $p$  values.

The random nature of the construction of the DLAs and the resulting noise in Figures 7 and 8 point to answers to some of the questions raised in the Introduction: It is clear that although the computation of an  $S(\sigma)$  value of a specific DLA is unique, the understanding and evaluation of the  $S(\sigma)$  are possible within the determination of statistical distribution of  $S(\sigma)$  values for a given set of parameters. This procedure is computationally costly, because it requires the analysis of many (a statistically signif-

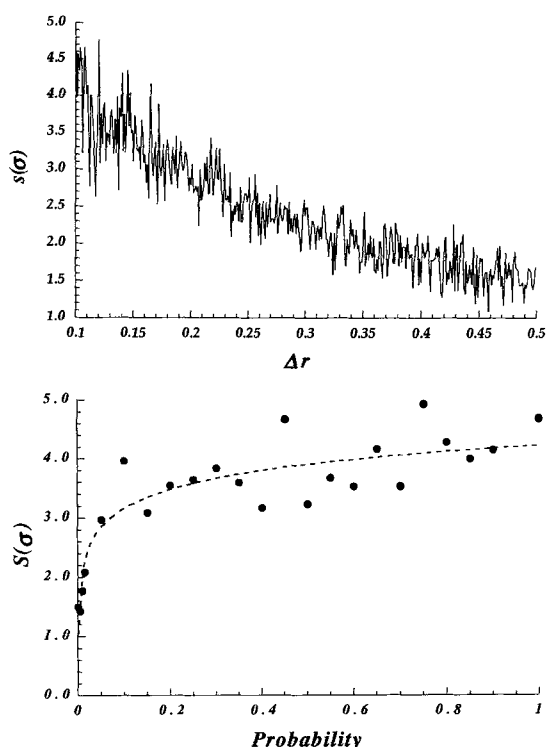


Fig. 8. Top: The dependence of  $S(\sigma)$  on the structural parameter  $\Delta r$  ( $N = 10^4$ ,  $\Delta a = 30^\circ$ ,  $p = 0.7$ ). Bottom: The dependence of  $S(\sigma)$  on the probability  $p$  of walking along the spiral line ( $N = 10^4$ ,  $\Delta a = 90^\circ$ ,  $\Delta r = 0.2$ ) (the dashed line serves to lead the eye and is a best fit to  $y = 4.21 + 1.06 \log x$ , with corr. coeff. of 0.890).

icant number) DLAs. Yet within the framework of this study, it was important to perform this analysis in order to demonstrate how to approach one of the key questions we raised in the Introduction, namely, whether the  $S(\sigma)$  values of inherent chiral DLAs are significantly higher than those obtained for incidental chiral objects and whether this type of analysis can provide a tool for distinguishing between these two principally different types of chirality. Figure 9 shows the frequency of  $S(\sigma)$  values for incidentally chiral DLAs and for two sets of inherently chiral ones; bell-shaped, relatively narrow, normal distributions are obtained (the parameters of which are given in the legend of Fig. 9). The inherently chiral DLAs are significantly outside the region of incidental chirality. Obviously, given other construction parameters, the normal-distribution bells may overlap in

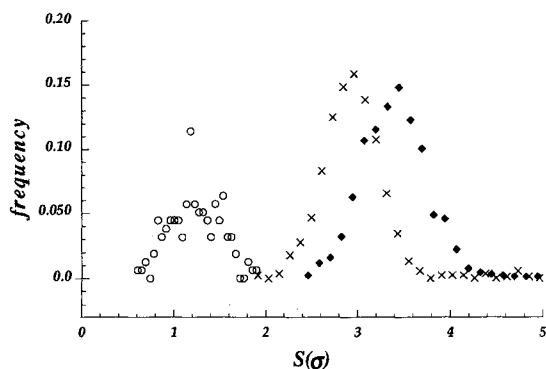


Fig. 9. The distribution of  $S(\sigma)$  values for a population of incidental DLAs (○) and for two sets (×, ●) of inherently chiral DLAs. ○: Number of DLA's ( $n_0$ ) = 158; ×:  $n_0 = 931$ ,  $\Delta a = 30^\circ$ ,  $\Delta r = 0.2$ ,  $p = 1.0$ ; ●:  $n_0 = 888$ ,  $\Delta a = 139^\circ$ ,  $\Delta r = 0.2$ ,  $p = 1.0$ . The bell-shape parameters, from left to right, are:  $S(\sigma) = 1.23 \pm 0.27$ ;  $2.93 \pm 0.37$ ;  $3.34 \pm 0.34$ .

part, and the distinction between incidental and inherent chirality may become statistically blurred.

The importance of establishing the minimum  $S(\sigma)$  value is seen in Figure 10. Here the  $S(\sigma)$  value is shown as the function of the orientation angle  $\theta$  of various reflection mirrors of the

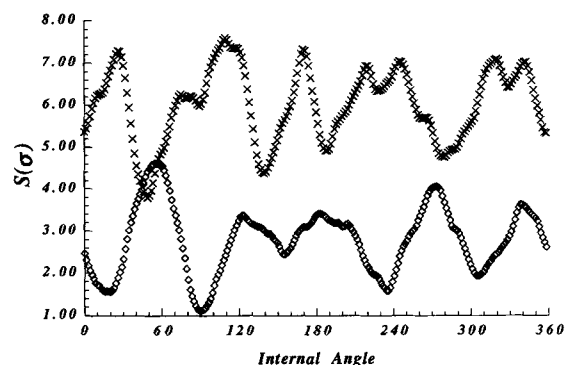


Fig. 10. The fluctuations in the chirality values as the orientation of the mirror line, around which  $\sigma$ -symmetrization is imposed, changes. Incidental (bottom line) and inherent (top line) cases are shown. The lowest values are the reported  $S(\sigma)$  (top:  $N = 10^4$ ,  $\Delta a = 90^\circ$ ,  $\Delta r = 0.2$ ,  $p = 1.0$ ; bottom:  $N = 10^4$ ,  $\Delta a = 90^\circ$ ,  $\Delta r = 0.2$ ,  $p = 0$ ).

symmetrized DLA passing through the origin (Fig. 5). The "spectrum" obtained is a fingerprint of a specific DLA and changes from one object to the next, for the same set of parameters. (Looking at this type of analysis one might perhaps propose that the average  $S(\sigma)$  is another representation of the chirality of the object; yet we recall that the basis of our methodology is to find the *minimum* distance that the vertices of a structure have to move to reach achirality; this means that while the average  $S(\sigma)$  may be high, it is sufficient to have one deep valley, indicating a specific inclination of  $\sigma$ , for which  $S(\sigma)$  will be significantly smaller than the average). Here too (Fig. 10), as in the case of Figure 9, the inherently chiral and the incidental DLA occupy different zones in the  $S(\sigma)$  vs.  $\theta$  plot, and only in such cases can one make the distinction between the two types. Minima in each of the two plots can be seen in Figure 10, which are at about the same depth—this calls for care in searching for the global minimum. In our case, this is achieved by dense screening over the inclination angles followed by even denser screening around the identified minimum. An important conclusion can be drawn from Figure 10: given a certain accuracy of computation, there may be more than one nearest symmetric shape (leading to the same  $S(\sigma)$  value); this, however, does not affect the very task of Equation (2), to find the minimum  $S(\sigma)$ .

Next we analyze properties of the DLAs associated with the resolution of measurement. As mentioned in the Introduction, unlike static structural properties of small molecules, where resolution is usually not an issue at all, this parameter becomes important in the analysis of large (random) objects. A first interesting question is whether the  $S(\sigma)$  value is affected by the density of sampling, in other words, whether one needs to use all the structural information available in order to obtain a reliable  $S(\sigma)$  value. The result, shown in Figure 11, is that 10% of the data points are enough for this purpose; this reflects the self-similarity of the object. This simplifies calculations significantly. A second question that should be asked in this context concerns the way in which the chirality content of a DLA change along the history of its growth, that is, with the number of particles that go to build it. The result (Fig. 12) is that  $S(\sigma)$  remains fairly constant from the "early childhood" of the DLA

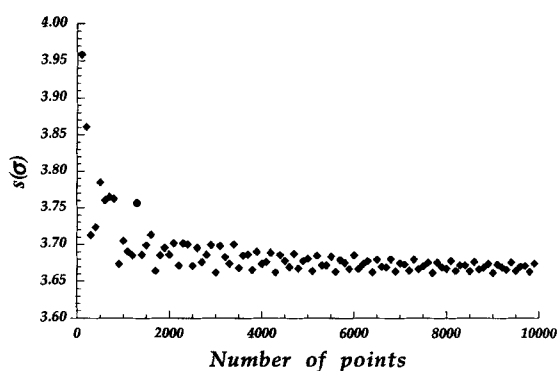


Fig. 11. The sensitivity of  $S(\sigma)$  to the sampling density of an inherently chiral DLA. Full density is  $N = 10^4$ , and it can be seen that  $S(\sigma)$  remains unaffected down to  $N \approx 2 \times 10^3$  (parameters as in Fig. 10, top)

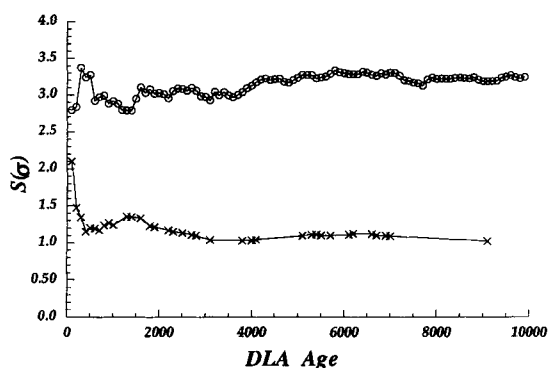


Fig. 12. The  $S(\sigma)$  values of inherently chiral DLAs (top) and incidental chiral DLAs (bottom) as the DLAs grow, that is, as  $N$  increases. Top:  $\Delta\alpha = 139^\circ$ ,  $\Delta r = 0.2$ ,  $p = 1.0$ ; bottom:  $p = 0$ .

( $N \approx 1.5 \times 10^3$  particles) up to  $N = 10^4$ . This is actually a manifestation of the self-similarity of these aggregates: brought down to the same scale, small and large DLA are indistinguishable from the point of view of their chirality. This scale invariance is also seen in Figure 13, where a set of DLAs of varying size is analyzed according to Equation (1). The scale invariance, both to global structure and to the chirality, is a unique feature of the chiral DLAs.

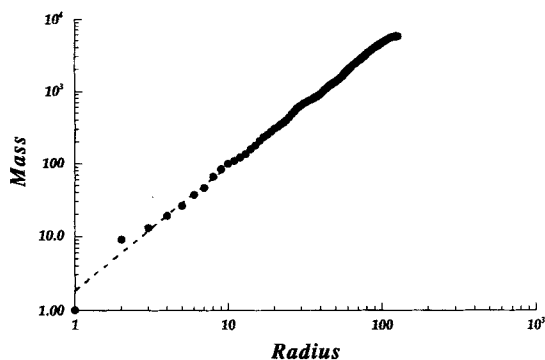


Fig. 13. Mass scaling analysis of the set of inherent DLAs in Figure 12. The apparent fractal dimension is 1.7 (parameters as in Fig. 10, top).

**2. Discussion and Proposed Answers to the Questions Raised in the Introduction:** The following conclusions emerge from Section 1:

1) For large, random chiral objects, an enantiomeric pair has meaning within a statistically large collection of objects.

2) Each member of this group is chiral in itself, and there are two types of answer as to what the enantiomer of a given member is: First, there is the enantiomer that is obtained by perfect reflection. As this enantiomer can be obtained only as a mirror image and never by actual repetition of the (chemical) process in which the original chiral object was obtained, we have proposed to term it a *virtual* enantiomer. Second, there is a *natural* enantiomer, which is any member of the set of objects obtained by repeating the construction in an enantiomeric way.

3) A last distinction must also be made within a set of enantiomers of the same handedness (for instance, the direction of spirality in our case): there are the natural *homochiral* members, and then there are virtual homochiral structures obtained by artificial “photocopying” of a structure.

4) The degree of chirality of a homochiral set can be expressed as a given mean  $S(\sigma)$  value with a variance (which at least in the case of DLAs has the characteristics of a normal distribution).

5) Having separate *enantiomeric populations* of right-handed<sup>[16]</sup> ( $R$ ) and left-handed ( $S$ ) objects, we define an *enantiomeric match* between two individual members of these populations as  $\Delta S = S(G_{\text{improper}})_R - S(G_{\text{improper}})_S$ . Intuitively one might perhaps guess that minimal  $\Delta S$ , or even  $\Delta S = 0$ , is indicative of approaching perfect reflectivity of the two structures. While this may be the case, it is not necessarily so, as different fine structural details may lead to different  $S(\sigma)$  values. In fact, *isochirality*, the property of having identical  $S(\sigma)$  values, does not necessarily indicate structural identity. The insensitivity of the continuous symmetry approach to details which lead to a certain  $S$  value is a manifestation of the globality (in the thermodynamic sense) of that parameter. In this sense,  $S(G)$  can serve as a *state function*.

6) The two enantiomers of a chiral object are classically labeled “left” or “right” under an agreed convention for these terms. Thus, our inherent chiral DLAs were labeled ( $R$ ) or ( $S$ ) according to the directionality of the underlying spiral.<sup>[16]</sup> However, one should bear in mind that labeling handedness is determined by a specific definition and that it is possible to construct chiral objects for which handedness cannot be assigned according to this definition (see, for example, the “*meso*” structure described in point 9 of this section).

7) Assigning handedness to incidental chirality is even more problematic, as already noted by Ruch<sup>[18]</sup> (who used potatoes to demonstrate the problem). A large assembly of incidentally chiral DLAs ( $p = 0$ ) can be divided into two enantiomeric populations, because “leftness” or “rightness” of each individual DLA is random. Specific rules can be constructed to help assign handedness to an incidental chiral DLA, but these will be so case-specific, that one wonders if one might not be better off reserving such assignments for when a specific need arises. One solution to this problem, however, is to use a small chiral probe structure (molecules) whose handedness can be assigned by standard rules (e.g., CIP rules<sup>[24]</sup>). The interaction of large chiral structures, such as our DLAs, with each of the two enantiomers of the small molecule will be different (diastereomeric), and this difference in interaction can be used for the assignment of handedness. We will show that this is indeed the case in a separate report.<sup>[25]</sup> In fact, only with an external small probe could we make a distinction between incidental and inherent chirality: the former shows statistical indifference to the two enantiomers of the probe.

8) As to the problem of the minimal feature required to dictate the chirality of the whole, one cannot adapt the approach used

for small molecules. In such a case, one looks both for local centers of chirality (e.g., tetrasubstituted atoms) and at the whole. In the case of the DLAs, the smallest chiral feature is composed of four pixels arranged in an L; there is a large number of these units in a DLA, and the influence the single entity on the chirality of the whole is negligible. A larger feature must be identified. In the case of the chiral DLAs we propose to use the smallest cluster for which the  $S(\sigma)$  value begins to stabilize (at the highest resolution), for instance, the chiral cores composed of  $N \approx 500$  particles in Figure 12. The nature of the minimal feature depends on the details of the analyzed structure; for the DLAs this means looking at the center of the object and not at the arms.

Another approach might be the search for minimum correlation length within which the object has the same handedness. Again, as in point 7, this can be established with various sizes of small molecular probes entering the DLA by diffusion or by mixing. We find that this correlation length is quite large, of the order of the radius of the DLA. We will elaborate on this finding in a subsequent report devoted to the interaction of chiral DLAs with small molecules.<sup>[25]</sup>

9) Let us now treat the chiral DLAs as building blocks and analyze the chirality of larger constructs. For instance, let us form dimers by attaching to one external point two DLAs from enantiomeric populations ( $R$ ) and ( $S$ ). As in the case of small molecules, there are three possible products, namely, ( $R,R$ ), ( $S,S$ ), and the *meso* ( $R,S$ ). If the selection of ( $R$ ) and ( $S$ ) DLAs is limited to natural ones, and not to virtual copies or reflections, then ( $R,R$ ) is in fact ( $R_1,R_2$ ) and an enantiomer of ( $S_1,S_2$ ), within the constraints of point 3. Interestingly, the *meso form is chiral* (in contrast to small molecules where it is achiral), and its  $S$  value need not be small. Another distinction from small molecules is that four (not one) *meso* combinations are possible: ( $R_1,S_1$ ), ( $R_2,S_2$ ), ( $R_2,S_1$ ), and ( $R_1,S_2$ ). Closely linked to the *meso* issue are the properties of a *racemic mixture*<sup>[9]</sup> of chiral DLAs. Its properties can be treated along the lines described so far.

10) Randomness and resolution dependency are the two main features of DLAs that require the extension of the concept of chirality. To clarify this point, let us consider an important class of inherently chiral, very large, *non-random* objects, namely, proteins. An exact enantiomer of a natural protein can be synthesized; a beautiful example is the synthesis of the unnatural enantiomer of an HIV protein.<sup>[26]</sup> Furthermore, the synthesis of proteins, unlike that of DLAs, is exactly reproducible, and the only variations in structure, which can also be reproduced, are in the folding of the chains. The common feature that DLAs share with proteins is that structural information is resolution dependent; this is a well-known aspect of protein studies.

11) Let us now return to Kelvin's definition of chirality,<sup>[1]</sup> in which he specifies that the "plane mirror [be] ideally realized". We are now in a position to lift this century-old restriction: with the possibility of scaling chirality, an ideal mirror becomes the limiting case in the rich arsenal of natural structures.

12) Coming back to Prelog's definition,<sup>[2]</sup> we asked whether the test for superimposability by translation and rotation could be extended to a third type of symmetry operation, namely, dilation. We have indeed shown that scale invariance (dilation symmetry) of  $S(\sigma)$  is one of the structural characteristics of a series of growing DLAs (Figs. 12 and 13). Actually, our definition of  $S$  takes care of this property, because the size of the analyzed structure is always normalized to 1. An important consequence of scale adjustment in the quantitative evaluation of  $S(\sigma)$  is that the chirality content is an *intensive* structural property. Yet, care

should be exercised in drawing this conclusion: if one wishes to evaluate the effects of (molecular) size on physical behavior (e.g., the absorption cross-section for circularly polarized light), such scaling should be removed.

## Conclusion

The classical definitions of chirality are quite suitable for small molecules; however, more general concepts must be introduced when dealing with large random objects. A generalized definition should refer to the fundamental inability to form an exact enantiomer, to the fact that chirality is resolution dependent, to incidental vs. inherent chirality, to the restrictive nature of an ideal mirror, and to the fact that superposition can be tested by criteria other than rotation–translation. We tentatively propose the following extended definition of chirality, which addresses many of these points (note that the classical definition that holds for small molecules is a limiting case):

*Chirality is the inability to make a structure coincide with a statistical realization of its mirror image; the probe-dependent measure of this inability is the chirality content of the structure.*

Beyond the conceptual analysis, a legitimate question concerns possible practical aspects of this approach. Separation of enantiomers on a chiral supports is one such practical example: each of the specific particles of the chiral chromatographic material, such as chirally derivatized silica, is different in detail from the other. It is a large collection of small chiral objects, randomly structured, yet with a characteristic chirality value, determined by a minimal unit, the derivatizing unit. The chromatographic interactions of the analyte with a given particle are not unique, but are determined by the distribution of orientations of the chiral ligands and by the diffusion, in and out, of the analyte, which, again, is dictated by the chirality of the surface.<sup>[27]</sup>

Finally, we note that the chiral DLAs we analyzed here, may be of relevance to domains beyond chemistry: spiral galaxies, spiral hurricane cloud formations, and spiral bacterial colonies<sup>[14]</sup> are but some examples of such domains.

## Appendices

### Appendix A—Vocabulary:

*Chirality measure*: the deviation of a chiral structure from exact achirality.

*Enantiomeric match*: the difference between the  $S$  values of two homochiral structures or within an enantiomeric pair, or between the mean  $S$  values of chiral populations.

*Enantiomeric population*: a collection of chiral structures, obtained by an identical chirally biased (random) process.

*Homochirality* is defined in a standard manner as the property of having the same handedness.

*Incidental chirality*: chirality that is the result of a random construction process.

*Inherent chirality*: chirality which is built-in owing to a chiral construction pathway.

*Isochirality*: chiral structures having the same chirality measure,  $S(G_{\text{improper}})$ , regardless of their handedness.

*Natural enantiomers*: chiral structures with opposite handedness, obtained by repeating the (random) procedure of construction with opposite chiral bias.

*Random chirality*: chirality resulting from a construction procedure that contains elements of randomness.

*Virtual enantiomer*: an exact mirror image of a random chiral structure, which in reality can never be obtained by repetition of the construction procedure with an opposite handedness.

**Appendix B—Properties of the Underlying Spirals:** Figures 14 and 15 and their captions summarize various properties of the underlying spirals and their  $S(\sigma)$  values. It can be seen (cf. Figs. 7 and 8) that these properties are preserved in the chiral DLAs.

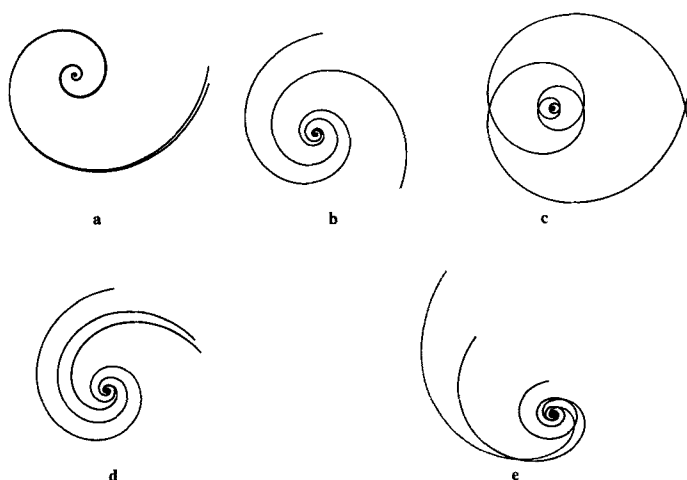


Fig. 14. Some properties of the underlying spirals. a) The fit between Equations (3) and (4) ( $\Delta r = 0.2$ ,  $\Delta a = 60^\circ$ ,  $K = -194$ ,  $C = 236$ ). b) Spirals having values of  $\Delta a$  and  $180^\circ - \Delta a$  are a rotated homochiral pair. See Figure 7, points a and b ( $\Delta r = 0.2$ ,  $\Delta a = 60^\circ$  and  $120^\circ$ ). c) Spirals with values of  $\Delta a$  and  $-\Delta a$  are an enantiomeric pair. See Figure 7, points a and d ( $\Delta r = 0.2$ ,  $\Delta a = 60^\circ$  and  $-60^\circ$ ). d) The effect of increasing  $\Delta r$  ( $\Delta r$  from center moving outwards: 0.1, 0.3, 0.5;  $\Delta a = 60^\circ$ ). e) The effect of increasing  $\Delta a$  ( $\Delta a$  from center moving outwards: 30, 45, 60;  $\Delta r = 0.2$ ).

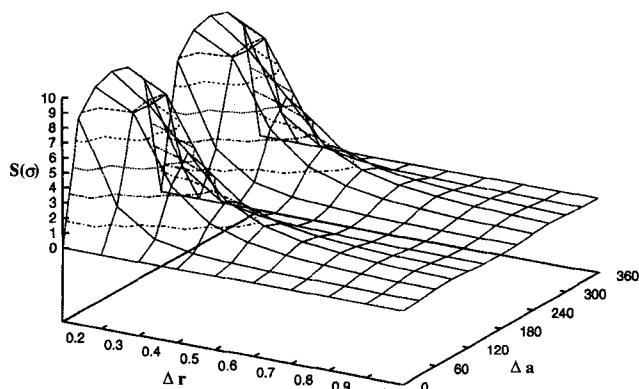


Fig. 15. The chirality measure of the underlying spirals as a function of the structural parameters  $\Delta r$  and  $\Delta a$  ( $N = 10^3$ ).

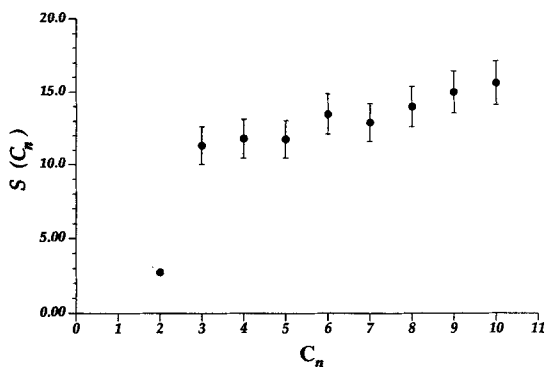


Fig. 16. The rotational symmetry content,  $S(C_n)$ , with respect to  $C_2 \rightarrow C_{10}$  of 158 DLAs (the distribution bars are shown; for  $C_2$  it is smaller than the dot size).

**Appendix C—Do DLAs have a Five-Fold Symmetry?** It was proposed by Arencodo et al. [29] that DLAs have an approximate  $C_5$  (and  $C_{10}$ ) symmetry. Our methodology allows the amount of symmetry in any element to be quantitatively evaluated [19], and we thus tested the hypothesis by analyzing 158 DLAs built from  $10^4$  particles, with respect to  $C_2 \rightarrow C_{10}$ . The results are shown in Figure 16: we find that the nearest symmetry is  $C_2$  and that the deviation for higher  $C_n$ 's is significantly larger.  $S(C_2)$  must be smaller or equal than any  $S(C_{2n})$ , because  $C_2$  is a subgroup of  $C_{2n}$ . At least by our method of analysis,  $C_5$  or  $C_{10}$  do not seem to have exceptional features.

**Acknowledgments:** We thank Prof. Sason Shaik, Yariv Pinto, and Yair Salomon for illuminating comments. D. A. is a member of the F. Haber Research Center for Molecular Dynamics and of the Farkas Center for Light Energy Conversion. This research was supported by the Israel Academy of Sciences and by the Robert Szold Institute for Applied Science of the P. E. F. Israel Endowment Fund.

Received: April 19, 1995 [F 124]

- [1] Lord Kelvin, *Baltimore Lectures*, 1884, 436 (cf. also *Baltimore Lectures*, Appendix H, 1904, 439); L. L. Whyte, *Nature*, 1958, 182, 198.
- [2] V. Prelog, *J. Mol. Catal.* 1975/6, 1, 159.
- [3] H. M. McConnell, *Annu. Rev. Phys. Chem.* 1991, 42, 171.
- [4] a) I. Mogi, S. Okubo, Y. Nakagawa, *J. Phys. Soc. Jpn.* 1991, 60, 3200; b) D. K. Schwartz, *Nature*, 1993, 362, 593; c) C. J. Eckhardt, N. M. Peachey, D. R. Swanson, J. M. Takacs, A. M. Kahn, X. Gong, J.-H. Kim, J. Wang, R. A. Uphaus, *J. Phys. Chem.* 1986, 90, 614; d) C. J. Eckhardt, N. M. Peachey, D. R. Swanson, J. M. Takacs, M. A. Khan, X. Gong, J.-H. Kim, J. Wang, R. A. Uphaus, *Nature*, 1993, 362, 614; e) D. P. Parazak, J.-Y. Uang, B. Turner, K. J. Steine, *Langmuir*, 1994, 10, 3787.
- [5] a) M. G. Green, B. A. Garetz, *Tetrahedron Lett.* 1984, 25, 1831; b) A. J. M. van Beijnen, R. J. M. Nolte, A. J. Naaktgeboren, J. W. Zwikker, W. Drenth, A. M. F. Hezemans, *Macromolecules*, 1983, 16, 1679.
- [6] a) P. Meakin in *The Fractal Approach to Heterogeneous Chemistry: Surfaces, Colloids, Polymers*, 3rd ed. (Ed.: D. Avnir), Wiley, Chichester 1992, chapt. 3.1.2; b) P. Meakin, *Heterog. Chem. Rev.* 1994, 1, 99; c) R. Jullien, R. Botet, *Aggregation and Fractal Aggregates*, World Scientific, Singapore, 1987.
- [7] For a large number of examples, see chapt. 3, in ref. [6a].
- [8] E. Ruch *Acc. Chem. Res.* 1972, 5, 49.
- [9] K. Mislow, P. Bickart, *Isr. J. Chem.* 1976/7, 15, 1.
- [10] H.-O. Peitgen, H. Jürgens, D. Saupe, *Fractals in the Classroom*, Springer, Berlin, 1992, Part II, p. 59; A. A. Chernikov, R. Z. Zagdeev, D. A. Usikov, G. M. Naslavsky, *Comput. Math. Appl.* 1989, 17, 17; P. Prusinkiewicz, A. Lindenmayer *The Algorithmic Beauty of Plants*, Springer, New York, 1990.
- [11] T. Nagatani, F. Sagues, *J. Phys. Soc. Jpn.* 1990, 95, 3447.
- [12] a) S. C. Müller, T. Plesser, B. Hess, *Naturwissenschaften* 1986, 73, 165; b) R. M. Weis, H. M. McConnell *Nature*, 1984, 310, 47; c) D. K. Kondepudi, R. J. Kaufman, N. Singh, *Science*, 1990, 250, 975.
- [13] R. D. Freimuth, L. Lam in *Modeling Complex Phenomena* (Eds. L. Lam, V. Naroditsky), Springer, New York, 1992, p. 303.
- [14] a) E. Ben-Jacob, H. Shmueli, O. Shochet, D. Weiss in *Growth Patterns in Physical Sciences and Biology* (Eds.: J. M. Garcia-Ruiz, E. Louis, P. Meakin, L. M. Sander), Plenum, New York, 1993, p. 11; b) E. Ben-Jacob, O. Shochet, A. Tenenbaum, I. Cohen, A. Czirok, T. Vicsek, *Fractals*, 1994, 2, 15.
- [15] J. H. van Esch, R. J. M. Nolte, H. Ringsdorf, G. Wildburg, *Langmuir*, 1994, 10, 1955.
- [16] We follow the convention of L. A. Bursill, J. L. Rouse, A. Needham in *Spiral Symmetry* (Eds.: I. Hargittai, C. A. Pickover), World Scientific, Singapore, 1992, p. 295. See also caption of Figure 2.
- [17] P. G. Mezey, *Shape in Chemistry*, VCH, Weinheim, 1993; P. G. Mezey, *J. Math. Chem.* 1992, 11, 27; *ibid.* 1991, 7, 39.
- [18] A. Janner, *Acta Crystallogr. Sect. A* 1991, 47, 577; *ibid.* 1992, 48, 884.
- [19] H. Zabrodsky, S. Peleg, D. Avnir, *J. Am. Chem. Soc.* 1992, 114, 7843.
- [20] H. Zabrodsky, S. Peleg, D. Avnir, *J. Am. Chem. Soc.* 1993, 115, 8278, 11, 656.
- [21] H. Zabrodsky, D. Avnir, *J. Am. Chem. Soc.* 1995, 117, 462.
- [22] H. Zabrodsky, D. Avnir, *Adv. Mol. Struct. Res.* 1995, 1, 1.
- [23] A. L. Loeb, W. Varney in ref. [16], p. 47.
- [24] R. S. Cahn, C. K. Ingold, V. Prelog, *Experientia*, 1956, 12, 81; V. Prelog, G. Halmchen, *Angew. Chem. Int. Ed. Engl.* 1982, 21, 567.
- [25] O. Katzenelson, unpublished results.
- [26] R. C. de L. Milton, S. C. F. Milton, S. B. H. Kent, *Science* 1992, 256, 1445 (Erratum: 1992, 257, 147).
- [27] In a preliminary study we found a monotonic correlation between the continuous chirality measure of a series of helixes and the efficiency of the separation of their enantiomers on a chiral chromatographic column (determined by Gil-Av et al. [28]).
- [28] F. Mikes, G. Boshart, E. Gil-Av, *J. Chem. Soc. Chem. Commun.* 1976, 99.
- [29] R. A. Hegstrom, D. K. Kondepudi, *Sci. Am.* 1990, 98.